Physics-Informed Machine Learning Models for Indoor Wi-Fi Access Point Placement

Guoli Yang, Shuyang Luo, Shichen Ji, Dongfang Cui, Aristeidis Seretis, Costas D. Sarris
The Edward S. Rogers Sr. Department of Electrical and Computer Engineering, University of Toronto
Toronto, ON, Canada
kevinguoli.yang@mail.utoronto.ca, shuyang.luo@mail.utoronto.ca, shichen.ji@mail.utoronto.ca,
dongfang.cui@mail.utoronto.ca, aris.seretis@mail.utoronto.ca, costas.sarris@utoronto.ca

***Abstract*—One of the main challenges in optimally placing indoor Wi-Fi access points in a complex indoor environment is the estimation of the received signal strength (RSS) given different access point locations. This paper proposes a deep learning approach, a modification to the classic Deep Convolutional Generative Adversarial Network (DCGAN), to generate accurate power maps for a specific indoor geometry. It has been demonstrated that this model consistently outperforms a benchmark ray-tracing simulator in efficiency, maintaining a comparable accuracy.**

I. Introduction

The placement of wireless access points (WAP) in an indoor environment requires some knowledge of the propagation characteristics in this environment. Based on this knowledge, WAP locations can be optimized to meet coverage and quality of service criteria for their network [1,2]. In this paper, we develop a Deep Convolutional Generative Adversarial Network (DCGAN) model to generate the power maps that indicate received signal strength (RSS) in an indoor environment based on given WAP locations. We introduce a unique data preprocessing approach to encode the raw data for the machine learning training purpose. This model can serve as an accurate simulation technique for optimizing WAP locations in complex indoor environments.

II. Methodology

A. Data Generation

A ray-tracing simulator based on the shooting and bouncing ray (SBR) method is used to generate RSS data at 1296 receiving points [3]. The generated RSS data would be further encoded into ground truth images for DCGAN training. The relative dielectric permittivity and conductivity of the walls in the ray-tracing simulator are set to 5 and 0.1 S/m respectively, as they correspond to materials often used in indoor environments. A 3D geometry model of the specified indoor environment is shown in Fig. 1.

B. Data Preprocessing

To better train the DCGAN model, we encode the data information into images where both magnitude and spatial information are maintained as RGB values of pixels. A data (ground truth) encoder, an input encoder, and a pixel decoder were implemented.

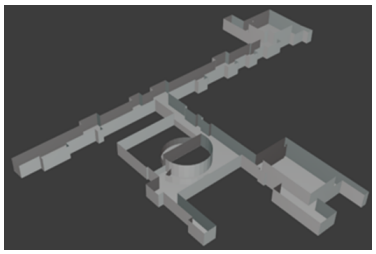

Fig. 1: The 3D geometry model of the indoor environment.

The data (ground truth) encoder encodes raw ground-truth RSS data into 36×36 pixel-encoded ground-truth images. RSS data at each receiving point are encoded as RGB color pixels. The pixel coordinate of each WAP directly corresponds to its physical coordinate. For each receiving point, the pixel coordinate is assigned dynamically based on its normalized RSS subtracted by its normalized physical (Euclidean) distance to the WAP, which we name this value as F_{recv}:

$$F_{recv} = \frac{RSS_{recv} - \min RSS}{\max RSS - \min RSS} - \frac{\|P_{recv} - P_{WAP}\|_2}{\max \|P - P_{WAP}\|_2} \quad (1)$$

where RSS_{recv} and P_{recv} are the RSS and physical coordinate at this particular receiving point, RSS and P are the RSS data and physical coordinate of any receiving point in the environment, and P_{WAP} is the physical coordinate of the WAP. The receiving points with higher F_{recv} would be assigned to the pixel coordinates closer to the pixel location of WAP. With this strategy, the spatial relations between receiving points and WAPs are kept. In addition, the encoded images would have common circular ripple patterns, which assists the learning process of our DCGAN model during training.

The input encoder encodes WAP locations into 36×36 pixel-encoded input images, as shown in Fig. 3. A binary mask is also applied on top of the pixel-encoded input image to emphasize the importance of WAP location in the input image.

The pixel decoder is a reversed process of the data (ground truth) encoder. It decodes pixel-encoded images generated by the DCGAN model into RSS data that would be used for further optimization processes of indoor Wi-Fi localization.

C. Deep Convolutional Generative Adversarial Network

1) U-Net: The generator is implemented using a 6-level U-Net to generate a high quality pixel-encoded image, where

the input is a pixel-encoded input image. The network has six down-sampling levels and six up-sampling levels. As shown in Fig. 2, each level has two 2D convolutional layers, with batch normalization and leaky ReLU in between [4]. Leaky ReLU is a rectified linear activation function with a small slope for negative values. In addition, each corresponding level is connected using skip-connections to preserve features and learn high-resolution details.

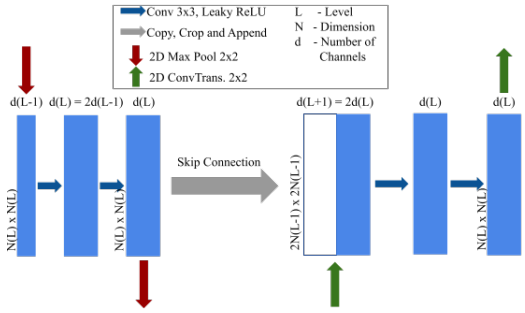

Fig. 2: Per-Level Architecture of U-Net Generator.

2) Convolutional Neural Network (CNN): The discriminator is a 4-layer CNN that classifies generated images and ground truth images as a binary classifier. It consists of four 2D convolutional layers followed by two linear layers. Following each convolutional layer, batch normalization and leaky ReLU function are used to stabilize the learning process.

3) Training: An adversarial strategy is used for the training, which allows both networks to be trained by optimizing against each other using the Minimax loss function [5]:

$$\mathcal{L}_{minimax} = \mathbb{E}_x[\log(D(x))] + \mathbb{E}_z[\log(1 - D(G(z)))] \quad (2)$$

While the generator is trained by the discriminator for the image generation task, the discriminator is trained to generate accurate classification results. Moreover, a dataset of 1296 pixel-encoded ground truth images is split into training, validation, and testing datasets with a ratio of 8:1:1.

III. DCGAN Results

To evaluate the DCGAN model's performance after training, we test the model on three datasets: training dataset, validation dataset, and testing dataset. We also use pixel-wise accuracy as a quantitative approach to evaluate the model:

$$A_{pixelwise} = 1 - \frac{\sum_{i=1}^{N_i} \sum_{p=1}^{N_{sp}} |p_t - p_g|}{N_i \times N_{sp} \times 255} \quad (3)$$

where N_i is the number of images and N_{sp} is the number of subpixels per image (3 subpixels per pixel in RGB images). Also, p_t and p_g are the value of target subpixel and generated subpixel respectively.

Tables I and II show the pixel-wise accuracy of the three different training dataset, and the average runtime of the ray-tracing simulator and our DCGAN model. Fig. 3 is a sample 36×36 pixel-encoded input image with its corresponding WAP location. Fig. 4 is the generated output image with the same size given the input image. It proves that the trained GAN model can successfully learn features from the corresponding ground truth image, shown in Fig. 5, as the color and shape pattern are well matched. Fig. 6 is the 128×128 power map with all generated RSS data rendered on the floor plan of the indoor environment. Fig. 7 is the legend that indicates the magnitude of RSS with corresponding color.

TABLE I: DCGAN Performance Evaluation: Accuracy.

Datasets	Training	Validation	Testing
$A_{pixelwise}(\%)$	79.00	78.84	78.02

TABLE II: DCGAN Performance Evaluation: Runtime.

	Ray-Tracing Simulator	DCGAN Model
Avg. Runtime (s)	43.03	0.42

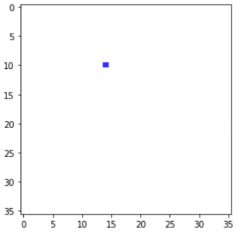

Fig. 3: Sample Pixel-Encoded Input Image.

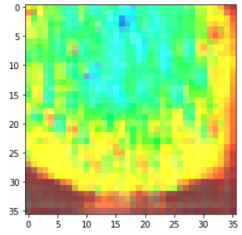

Fig. 4: Generated Output Image.

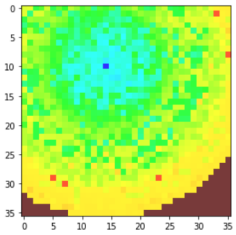

Fig. 5: Corresponding Ground Truth Image.

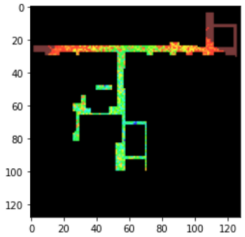

Fig. 6: Power Map with the Floor Plan.

Fig. 7: Received Power [dBm].

References

[1] F. Firdaus, N. A. Ahmad, and S. Sahibuddin, "Accurate Indoor-Positioning Model Based on People Effect and Ray-Tracing Propagation," *Sensors*, vol. 19, no. 24, p. 5546, Dec. 2019.

[2] D. Lymberopoulos and J. Liu, "The Microsoft indoor localization competition: Experiences and lessons learned", *IEEE Signal Processing Magazine*, vol. 34, no. 5, pp.125-140, 2017.

[3] F. Fuschini et al., "Ray tracing propagation modeling for future small-cell and indoor applications: A review of current techniques," *Radio Science*, vol 50, no. 6, pp. 469-485, 2015.

[4] O. Ronneberger, P. Fischer and T. Brox, "U-Net: Convolutional Networks for Biomedical Image Segmentation", *Computer Science Department and BIOSS Centre for Biological Signalling Studies*, University of Freiburg, Germany, 2015.

[5] I. Goodfellow et al., "Generative Adversarial Networks", arXiv.org, 2021. [Online]. Available: https://arxiv.org/abs/1406.2661. [Accessed: 28- Mar- 2021].